Journal of Electrical Engineering & Technology Vol. 7, No. 5, pp. 745~752, 2012 **745**
http://dx.doi.org/10.5370/JEET.2012.7.5.745

Optimum Design of Transverse Flux Machine for High Contribution of Permanent Magnet to Torque Using Response Surface Methodology

Jia Xie†, Do-Hyun Kang, Byung-Chul Woo**, Ji-Young Lee**, Zheng-Hui Sha*** and Sheng-Dun Zhao***

Abstract – Transverse flux machine (TFM) has been proved to be very suitable for high-torque, low-speed, and direct-drive situation in industry. But the complex structures and costly permanent magnets (PMs) are two key limitations of its wide range of applications. This paper proposes a new claw pole TFM (ACPTFM) which features an assembled claw pole stator and using the lamination steels material to overcome the complex structures. By combining response surface methodology (RSM) with design of experiment, an optimum design method is put forward to improve the PM's contribution to the torque in order to save the PM's amount. The optimum design results demonstrate the validity of the proposed optimum design method and the optimized model. Eventually, the finite-element analysis (FEA) calculation method, which is used in the optimization process, is verified by the experiments in a prototype.

Keywords: Claw pole transverse flux machine, Contribution of permanent magnet to torque, Optimum design, Response surface methodology

1. Introduction

Transverse flux machine (TFM) has a number of characteristics distinguished from other electric machines. Firstly, it has a magnetic flux path with sections where the flux is transverse to the direction of motion. This is different with longitudinal flux machine that the magnetic flux path and the direction of motion are in the same plane. The novel structure of the magnetic flux path leads to the decoupling of the magnetic and electric loading in TFM, thus makes it possible to achieve higher force densities by increasing electric and magnetic loading, respectively [1]. Secondly, TFM can be produced with many pole pairs. Thereby, a low-speed characteristic can be realized. Furthermore, many pole pairs make it possible to apply flux-concentrating rotor structure to improve the flux densities in the air gap. Thirdly, each phase of TFM is independent, so there is no electromagnetic coupling between them. This feature makes TFM easy to fabricate with many phases to achieve high torque and reduce the torque ripples. Accordingly, TFM is particularly suitable for high-torque, low-speed, and direct-drive applications.

TFMs have been considered as viable candidates to be applied in many direct-drive fields, such as electromagnetic launch [2], railway traction [3], vehicle electric propulsion [4], direct drive robots [5], energy conversion [6], wind turbine [7], and electromagnetic launcher [8]. These applications show that TFMs have salient advantages in the field of the direct drive. However, some disadvantages often plague the development of TFMs. Especially, the complex structures of the TFMs result in a lot of difficulties in machine assembly and high manufacturing costs. Meanwhile, permanent magnet (PM) which must be used in TFMs is expensive. Therefore, this paper proposes a new claw pole TFM (ACPTFM) which manufactures for high power applications to perform direct drive. ACPTFM features an assembled claw pole stator and the lamination steels material which realize the machine with simple structure, simple manufacturing processes, low iron losses, and high magnetic permeability. In order to achieve rational structure dimensions of each part in the machine, an optimum method called combined response surface methodology (RSM) and design of experiment was applied. This method can achieve excellent performance and low costs by optimizing multiple design variables of ACPTFM.

Design of experiment can be regarded as a carefully arranged experiment procedure. The purpose of design of experiment is two-fold. The first is to make the experiment procedure reasonable and can be conducted orderly; and the second is to get adequate and reliable information by minimal number of experiments [9]. RSM is a set of statistical and mathematical techniques. In RSM, a polynomial model is constructed to represent the relationship between the performance and multiple design variables. The ultimate goal of RSM is to find the best fitted response of the physical system through real

† Corresponding Author: Dept. of Electromechanical Engineering, Xi'an Jiaotong University, China. (xiejia.min@stu.xjtu.edu.cn)
* Dept. of Electromechanical Engineering, Xi'an Jiaotong University, China. (sdzhao@mail.xjtu.edu.cn)
** Dept. of Electric Motor Research Center, Korea Electrotechnology Research Institute, Korea.(dhkang@keri.re.kr; bcwoo@keri.re.kr; jylee@keri.re.kr)
*** School of Mechanical and Materials Engineering, Washington State University, USA.(zhenghui.sha@email.wsu.edu)
Received: September 14, 2011; Accepted: May 4, 2012

experiment or computer simulation [10]. Research and application of RSM as an optimization method have been carried out in many fields [11-13]. As a summary, RSM combined with design of experiment is regarded as an ideal method to perform the optimum design for ACPTFM.

The paper is organized as follows. Section II presents the analysis model and design variables. Meanwhile, ACPTFM is proposed and the parameters are introduced. In section III, the optimization method is presented. RSM combined with design of experiment is applied and the fitted model for three design variables is established. Section IV gives the optimum design results. The contribution of PM to the torque is improved, which validates the effectiveness of the optimization method. In Section V, experiments are done to verify the finite-element analysis (FEA) calculation method used in the optimization process in an actual prototype. Finally, section VI concludes this work.

2. Analysis Model and Design Variables

2.1 Analysis model – ACPTFM

The claw pole TFM highlights both the simplicity of the single-sided TFMs and the high performances of the double-sided ones. It allows an easy assembly and any number of axially arranged phases [14]. However, the stator often needs to use isotropic materials to provide the three-dimension (3-D) flux paths in the claw pole TFM. The isotropic materials will reduce the performance of the machine and make the manufacture of the machine fairly complex. In practice, the soft magnetic composite (SMC) is often adopted in the machine because it is isotropic. In addition, SMC tends to have lower eddy currents than those typically used in conventional electrical drives when the machine is operated at high supply frequencies (100 kHz or more) [15]. This feature is suitable for high speed machine. However, SMC has some major disadvantages, such as low magnetic permeability resulting from low saturation flux density, high hysteresis losses at low supply frequencies, low mechanical strength which makes it difficult to produce high force densities, and it has not competitive cost-effectiveness with cheaper lamination steels. Since the machine designed in this paper is for the low speed applications, the supply frequencies are impossible to reach 100 kHz.

Therefore, we propose the ACPTFM which has the claw pole structure and uses the lamination steels material to promote the advantages of the claw pole TFM and overcome the disadvantages of SMC. In order to obtain 3-D magnetic flux paths, the stator core of ACPTFM must be assembled because of using the lamination steels material. Fig. 1 shows the single-phase configuration of ACPTFM and its 3-D magnetic flux paths. Single-phase ACPTFM consists of an assembled claw pole stator, a flux-concentrating rotor, and a ring stator winding.

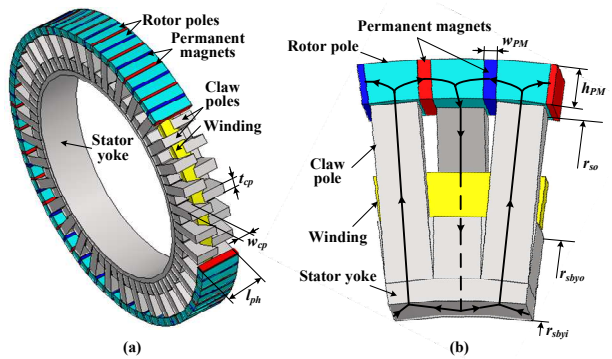

Fig. 1. Single-phase configuration of ACPTFM: (a) Cut away of ACPTFM showing claw poles and winding; (b) 3-D magnetic flux paths

In the claw pole stator as shown in Fig. 1, the stator yoke is made of the first laminated stack of metal sheets whose laminations are stacked in an axial direction, and the stator claw poles are made of the second laminated stack of metal sheets whose laminations are stacked in a tangential direction. Each sheet of the stator yoke is annular and the square holes evenly distribute along the circumferential direction in the surface of the sheet. The stator arrangement comprises an annular stator yoke as well as a plurality of stator claw poles, one half of the stator claw poles (36 pieces) being inserted into the square holes of the stator yoke from one end face of the stator yoke and the other half of the stator claw poles being inserted into the square holes from the opposite end face of the stator yoke. As a result, the conduction of the magnetic field linearly passes through the stator claw poles and linearly passes through the stator yoke between the two stator claw poles so that can realize the 3-D magnetic flux paths. And the individual component of the stator can be made of well-know stamped sheet metal and lamination techniques which make the manufacturing processes simple and reduce the costs. Flux-concentrating rotor is consisted of two magnetic polarities by PMs, N and S, alternatively arranged along the circumferential direction. It can produce high air-gap flux densities. The rotor poles are made of solid carbon steel for easy assembling.

As shown in Fig. 1(b), the fluxes flow through the magnetic circuit within the real 3-D paths. The fluxes circumferentially pass through two successive magnets into the rotor north poles and then radially across the air gap into the stator south claw poles, then round the stator back yoke and into the two adjacent teeth on the other side of the stator which is considered as stator north claw poles. Then the fluxes radially up these stator north claw poles and back across the air gap into the other side adjoining rotor teeth (rotor south poles). Finally, the fluxes circumferentially return to the buried PMs along two opposite paths. Once the current is energized, the torque resulting from the interaction between the coil MMF and the permanent magnetic field will produce motion in the

circumferential direction. This is the principles of the torque generation of ACPTFM. Since it is well known that single-phase TFM has a dead point of torque, we use the combination of three phases, which means that the stator teeth of two adjacent phases are shifted by a 60°-electrical angle and the rotor teeth are aligned, to produce continuous torque. The three phases can also effectively reduce the torque ripples of ACPTFM.

2.2 Design variables

According to practical issues, some design parameters of ACPTFM are fixed, see Table 1. Some basic dimensions can be sized by applying the flux conservation law and are also included in Table 1. The flux conservation law is an approximate method which only considers the major magnetic flux path. Therefore, the crucial parameters should be determined by accurate methods in which the major magnetic flux path and the leakage one should be all considered. Additionally, the 3-D magnetic flux path as shown in Fig. 1(b) requires 3-D analysis. As a result, accurate results should be gained through 3-D FEA.

Table 1. Parameters of ACPTFM

Parameters	Quantities
Rated power (kW)	29
Rated voltage (v)	514
Rated MMF (AT)	1800
Rated torque (Nm)	2700
Range of speed for constant torque (rpm)	0-100
Range of speed for constant power (rpm)	100-500
Maximum speed (rpm)	800
Number of phases	3
Number of pole pairs	36
Stator outer radius: r_{so} (mm)	275
Stator back yoke outer radius: r_{sbyo} (mm)	231
Stator back yoke inner radius: r_{sbyi} (mm)	199
Single-phase axial length: l_{ph} (mm)	78
Claw pole thickness: t_{cp} (mm)	18
Claw pole arm width: w_{cp} (mm)	24
Air gap length (mm)	1
Magnet material	NdFeB

In this study, the crucial parameters are magnet width w_{PM} (dv_1), magnet height h_{PM} (dv_2), and overlap between adjacent stator teeth (dv_3) because they are very sensitive to the torque of the machine and the amount of the used PMs. Therefore, dv_1, dv_2, and dv_3 are selected as the design variables to optimize the performance of ACPTFM. In this paper, the overlap between adjacent stator teeth is defined as zero when the tips of the stator teeth just reach the axial centre of the stator yoke and it is defined as 100% when the tips of the stator teeth reach the end face of the stator yoke.

3. Optimum Design

3.1 Optimum design process

Fig. 2 shows the optimum design process of ACPTFM using RSM. As described in section 2.2, the selected design variables are dv_1, dv_2, and dv_3. Table 2 shows the design variables and levels. The design variables in zero level are the values of the initially designed ACPTFM. The design variables in +α level and -α level, which are determined by possible values of the three design variables, decide the maximum and minimum respectively.

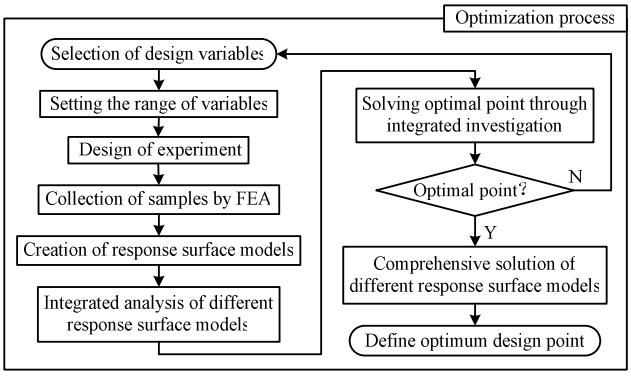

Fig. 2. Optimum design process of ACPTFM using RSM

3.2 Design of experiment

Design of experiment for fitting second-order response model must involve at least three levels of each variable. Therefore, central composite design (CCD) experimental design method is adopted to meet the requirements of fitting second-order response model [9]. CCD is obtained by increasing some sample points based on the 2^k (k is the number of the design variables.) full factorial design or fractional factorial design. The increased sample points are composed of some middle values points and $2k$ points which are in the coordinate axis and from the middle values points +α and -α, respectively. In order to obtain an orthogonal CCD, α is defined as 1.216 in this paper. The corresponding values of the design variables are shown in Table 2.

Table 3 shows the array of 2^3 CCD, which is determined by the number of the design variables and their levels. Three design variables (three levels) need 27 combinations by full factorial design. However, CCD needs 15 combinations as shown in Table 3. The optimum result is

Table 2. Design variables and levels

Design variables	Levels of design variables				
	-α	-1	0	+1	+α
dv_1 (mm)	0.92	2	7	12	13.08
dv_2 (mm)	0.38	2	9.5	17	18.62
dv_3 (%)	-6.49	0	30	60	66.49

almost similar to full factorial design. The calculation time is saved using CCD.

Table 3. Array of 2^3 CCD

Experiment No.	dv_1 (level)	dv_2 (level)	dv_3 (level)
1	-1	-1	-1
2	+1	-1	-1
3	-1	+1	-1
4	+1	+1	-1
5	-1	-1	+1
6	+1	-1	+1
7	-1	+1	+1
8	+1	+1	+1
9	0	0	0
10	-α	0	0
11	+α	0	0
12	0	-α	0
13	0	+α	0
14	0	0	-α
15	0	0	+α

3.3 Response surface methodology

RSM is applied to seek the relationship between multiple design variables and response in interested area through statistical fitting method, which is based on the investigation data from the designed machine. In this paper, a second-order response model is established. An approximately polynomial model is commonly used for a second-order response function, which is expressed as [10]

$$y = \beta_0 + \sum_{i=1}^{k} \beta_i x_i + \sum_{i=1}^{k} \beta_{ii} x_i^2 + \sum_{i<j}^{k} \beta_{ij} x_i x_j + \varepsilon \quad (1)$$

where x represents the design variables, and β is the regression coefficients for design variables, and ε denotes a random error treated as statistical error. The observation response vector $\mathbf{Y}$ of function y can be written as matrix notation

$$\mathbf{Y} = \mathbf{X}\boldsymbol{\beta} + \boldsymbol{\varepsilon} \quad (2)$$

where $\mathbf{X}$ is the matrix notation of the independent design variables, and $\boldsymbol{\beta}$ is the vector of the regression coefficients, and $\boldsymbol{\varepsilon}$ is the vector of the random errors. The least square method is used to estimate unknown coefficients $\boldsymbol{\beta}$. The estimated vector of $\boldsymbol{\beta}$ is written as

$$\hat{\boldsymbol{\beta}} = (\mathbf{X}'\mathbf{X})^{-1}\mathbf{X}'\mathbf{Y} \quad (3)$$

where $\mathbf{X}'$ is the transpose matrix notation of the design variables. Then the fitted response vector $\hat{\mathbf{Y}}$ is expressed as

$$\hat{\mathbf{Y}} = \mathbf{X}\hat{\boldsymbol{\beta}}. \quad (4)$$

In this paper, the second-order fitted model (4) is used as the objective function. In order to achieve the high contribution of PM to the torque, two objective functions are adopted. F_{obj1} is the average torque over one pole pitch of the single phase in ACPTFM, and it is used to investigate the torque variation; F_{obj2} is the ratio of the PM volume to the average torque, and it is used to express the contribution of PM to the torque.

4. Optimum Design Results

As mentioned above, with the three design variables dv_1, dv_2 and dv_3, CCD is required to perform 15 experiments, see Table 4. The 3-D static magnetic field is analyzed for each experiment. The average torque and the ratio of the PM volume to the average torque are calculated as shown in Table 4. The torque profile of experiment results according to variation of the design variables are simulated by 3-D FEA and are shown in Fig. 3.

Table 4. Simulation experiment results

Experiment No.	dv_1 (mm)	dv_2 (mm)	dv_3 (%)	Average torque (Nm)	PM volume /Average torque (mm^3/Nm)
1	2	2	0	107.6	208.77
2	12	2	0	176.78	762.42
3	2	17	0	594.73	321.06
4	12	17	0	1261.92	907.88
5	2	2	60	190.16	118.13
6	12	2	60	310.38	434.25
7	2	17	60	584.68	326.58
8	12	17	60	1289.95	881.99
9	7	9.5	30	920.53	405.71
10	0.92	9.5	30	285.01	172.22
11	13.08	9.5	30	1032.18	676.09
12	7	0.38	30	43.18	345.94
13	7	18.62	30	1292.65	566.27
14	7	9.5	-6.49	867.75	430.38
15	7	9.5	66.49	905.52	412.43

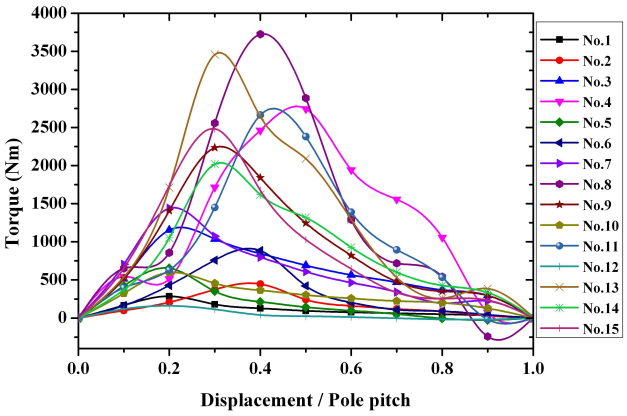

Fig. 3. Torque profile of simulation results

After getting the experimental data by 3-D FEA, the two objective functions which are used to draw response surface are extracted using (3) and (4). The purpose of this paper is to achieve high contribution of PM to the torque. This is performed by minimizing the objective function F_{obj2} and maintaining F_{obj1}. The two objective functions, namely the fitted models, for the three design variables are shown as below

$$\begin{aligned} F_{obj1} = & -305.3368 + 99.8189dv_1 + 84.8185dv_2 \\ & + 2.305dv_3 - 6.7689dv_1^2 - 2.8963dv_2^2 \\ & - 0.0167dv_3^2 + 3.9735dv_1dv_2 + 0.0818dv_1dv_3 \\ & - 0.1051dv_2dv_3 \end{aligned} \quad (5)$$

$$\begin{aligned} F_{obj2} = & 197.0216 + 30.0821dv_1 - 15.5185dv_2 \\ & - 3.7068dv_3 + 1.1372dv_1^2 + 0.8896dv_2^2 \\ & + 0.0295dv_3^2 + 0.9082dv_1dv_2 - 0.2241dv_1dv_3 \\ & + 0.2214dv_2dv_3 . \end{aligned} \quad (6)$$

It is necessary to examine the fitted model to ensure that it can provide an adequate approximation for the response model. Analysis of variance is applied to investigate the precision of the fitted model. The coefficient of multiple determinations R^2 and its adjustment coefficient R^2_{adj} are utilized to evaluate the accuracy of the fitted model in this paper. R^2 and R^2_{adj} for two responses are F_{obj1} (0.975 and 0.971) and F_{obj2} (0.981 and 0.978). The coefficients are fairly high, which shows that the fitted model provide an adequate approximation for the response model.

Fig. 4 shows the response surface for objective functions F_{obj1} average torque and F_{obj2} PM volume/average torque. The rated torque of ACPTFM is 2700 Nm, so the rated torque of the single phase in the machine is 900 Nm. Fig. 4 (a) indicates that in order to get 900 Nm average torque, the magnet width dv_1 should be in the range of 4.5 mm to 6.5 mm and the magnet height dv_2 should be in the range of 9.5 mm to 14 mm. And when dv_1 and dv_2 are in such range, the objective function F_{obj2} has a minimum. Fig. 4(b) and (c) show that F_{obj1} is not sensitive to the overlap dv_3, which shows that the values of the optimal point of dv_1 and dv_2 are in the range described above indeed. At the same time, it can be seen from Fig. 4(b) and (c) that F_{obj2} has a minimum when dv_1 and dv_2 are in the above range though F_{obj2} has small changes in these ranges.

Fig. 4 predicts the small existence range of the optimal point, which is useful for further optimum design to determine the optimal point ultimately. Under the condition that the single-phase rated torque is 900 Nm, the design variable dv_2 is calculated through objective function F_{obj1} when the design variables dv_1 and dv_3 are given. Then, substituting dv_1, dv_2, and dv_3 into objective function F_{obj2}, we obtain the new response surface and contour of the ratio of the PM volume to the average torque as shown in Fig. 5. In the predicted small range of dv_1, dv_2 and dv_3, the optimal point is determined eventually.

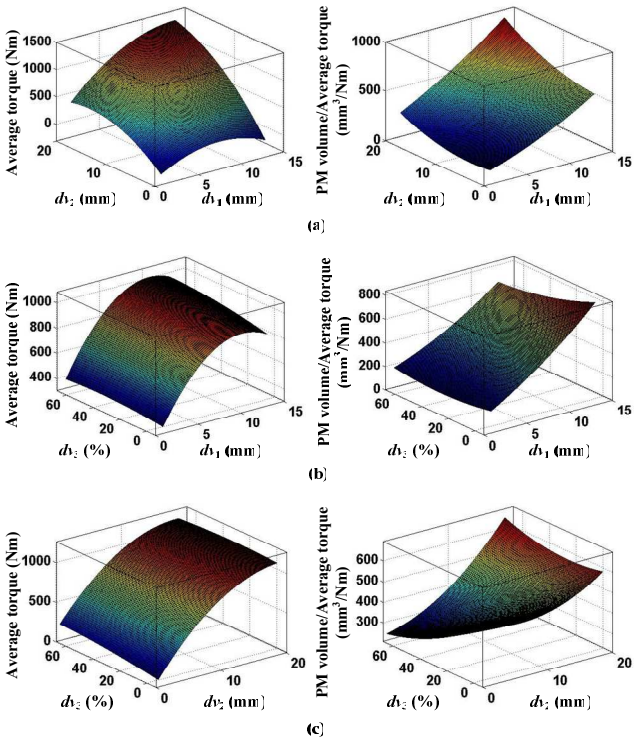

Fig. 4. Response surface for objective functions F_{obj1} average torque and F_{obj2} PM volume/average torque. The MMF applied in the stator winding is 1800 AT: (a) dv_3 = 30 % (0 level); (b) dv_2 = 9.5 mm (0 level); (c) dv_1 = 7 mm (0 level)

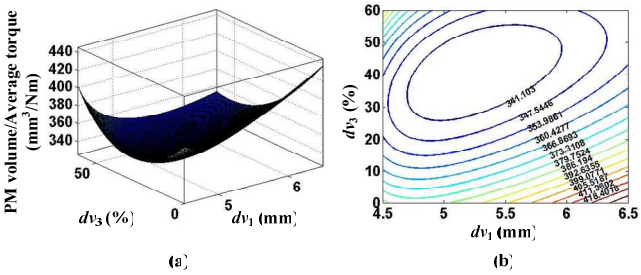

Fig. 5. Response surface and contour for the objective function F_{obj2} PM volume/average torque at average torque = 900 Nm. The MMF applied in the stator winding is 1800 AT: (a) Response surface; (b) Contour

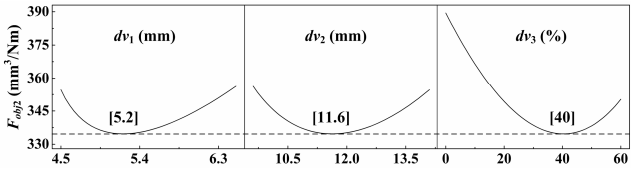

Fig. 6. Optimized point

Fig. 6 shows the optimal point and the contour lines. The optimal design point is finally decided when the magnet width dv_1 equals to 5.2 mm, the magnet height dv_2 equals

to 11.6 mm, and the overlap between adjacent stator teeth dv_3 equals to 40 %. Table 5 lists the optimum level and optimal point. Table 6 shows the comparison of the initial model and the optimized one. Compared with the initial model, the optimum model achieves a decrease of 10.71 % in the ratio of the PM volume to the average torque. This relatively improves the contribution of PM to the torque. And the average torque of the optimum model has almost no changes compared to that of the initial model.

Table 5. Optimum level and size

Item	Design variables		
	dv_1	dv_2	dv_3
Optimum level	-0.36	0.28	0.333
Optimum size	5.2 mm	11.6 mm	40 %

Table 6. Comparison of initial model and optimized model

Model	Average torque (Nm)	PM volume/Average torque (mm^3/Nm)
Initial	920.53	405.71
Optimum	929.49	364.45
Variation (%)	0.97	-10.17

5. Experiment for Verifying the 3-D FEA Calculation Method

As mentioned above, in the optimum design process, the experimental samples are obtained from 3-D FEA calculation method. Thereby, it is necessary to verify the accuracy of the FEA calculation method. An actual prototype is applied to implement the 3-D FEA calculation method and experiments in the rotate model, and then a comparison is done to investigate the difference between two methods. The actual prototype is shown in Fig. 7. And the comparison is shown in Fig. 8.

The actual prototype adopts outer-rotor structure. Its stator and the rotor are made of the laminated stack of metal sheets, and the stator also uses the claw pole technique. The structure of the actual prototype is similar to the optimized one. In order to verify the FEA calculation method in a large range, the applied current for experiment varies between 3.6 A and 7.2 A. The close static torque profiles and a very acceptable deviation within 2% of averaged static torque verified the accuracy of FEA calculation method applied in the optimum design process.

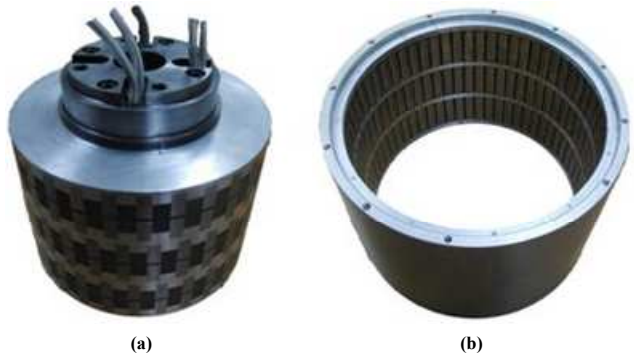

Fig. 7. Actual prototype: (a) Stator; (b) Rotor

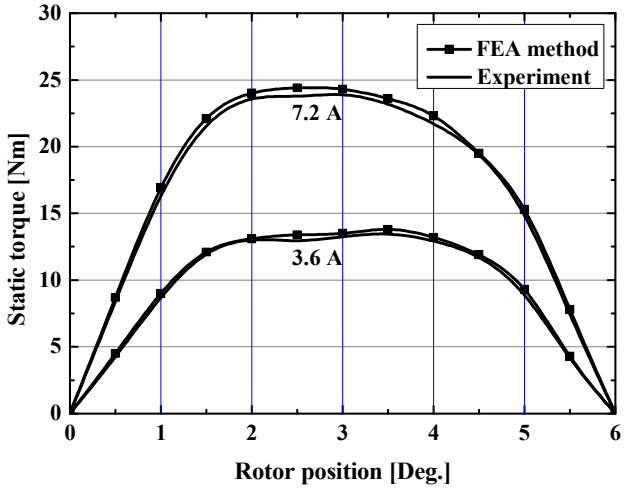

Fig. 8. Comparison between experiment and FEA calculation method

6. Conclusion

In this paper, a novel claw pole TFM – ACPTFM is proposed. ACPTFM has assembled claw pole stator and utilizes the lamination steels material to overcome the complex structures and improve the performance of the machine, An optimum design method using RSM is presented to design ACPTFM in order to improve the contribution of PM to the torque. The optimum design is performed by maintaining the average torque while minimizing the ratio of the PM volume to the average torque. By implementing the optimization, the amount of the PM is reduced without compromising the performance of the machine. Finally, a prototype is applied to verify the validity of the FEA calculation method which is used in the optimization process. The results show that the optimum design is valid and prove that the optimization and the optimized model are successful.

References

[1] A.Y. Chen, R. Nilssen and A. Nysveen, "Performance comparisons among radial-flux, multistage axial-flux, and three-phase transverse-flux PM machines for

downhole applications," *IEEE Trans. Ind. Appl.*, vol.46, no.2, pp.779-789, Mar./Apr. 2010.
[2] J.B. Zou, Q. Wang and Y.X. Xu, "Influence of the permanent magnet magnetization length on the performance of a tubular transverse flux permanent magnet linear machine used for electromagnetic launch," *IEEE Trans. Plasma Science*, vol.39, no.1, pp.241-246, Jan. 2011.
[3] D.H. Kang, Y.H. Chun and H. Weh, "Analysis and optimal design of transverse flux linear motor with PM excitation for railway traction," *in Proceedings of IEE Electr. Power Appl.*, London, UK, pp.493-499, Jul. 2003.
[4] A. Masmoudi and A. Elantably, "An approach to sizing high power density TFPM intended for hybrid bus electric propulsion," *Electr. Power Components and Systems*, vol.28, no.4, pp.341-354, Apr. 2000.
[5] A. Babazadeh, N. Parspour and A Hanifi, "Transverse flux machine for direct drive robots: modeling and analysis," *in Proceedings of IEEE Conference on Robotics, Automation and Mechatronics*, Singapore, pp. 376-380, Dec. 2004.
[6] H. Polinder, B.C. Mecrow, A.G. Jack, P.G. Dickinson and M.A. Mueller, "Conventional and TFPM linear generators for direct-drive wave energy conversion," *IEEE Tran. Energy Conversion*, vol.20, no.2, pp.260-267, Jun. 2005.
[7] D.J. Bang, H. Polinder, G. Shrestha and J.A. Ferreira, "Design of a lightweight transverse flux permanent magnet machine for direct-drive wind turbines," *in Proceedings of IEEE Ind. Appl. Society Annual Meeting*, Edmonton, Alberta, Canada, pp.1-7, Oct. 2008.
[8] M. Zhao, J.M. Zou, Y.X. Xu, J.B. Zou and Q. Wang, "The thrust characteristic investigation of transverse flux tubular linear machine for electromagnetic launcher," *IEEE Trans. Plasma Science*, vol.39, no.3, pp.925-930, Mar. 2011.
[9] D.C. Montgomery, *Design and Analysis of Experiments*: 7th ed., New York: Wiley, 2008.
[10] A.I. Khuri and J.A. Cornell, *Response Surfaces: Designs and Analyses*: New York: Marcel Dekker, 1996.
[11] C. Yuan, B.G. Liu and C.G. Chen, "Optimization of preparation process of hydroxypropyl-β-cyclodextrin by response surface methodology," *in Proceedings of International Conference on Challenges in Environmental Science and Computer Engineering*, Wuhan, China, pp.26-28, Mar. 2010
[12] S.I. Kim, J.P. Hong, Y.K. Kim, H. Nam and H.I. Cho, "Optimal design of slotless-type PMLSM considering multiple responses by response surface methodology," *IEEE Trans. Magn.*, vol.42, no.4, pp.1219-1222, Apr. 2006.
[13] D.K. Hong, B.C. Woo and D.H. Kang, "Application of fractional factorial design for improving performance of 60 W transverse flux linear motor," *J. Appl. Phys.*, vol.103, no.7, pp. 07F120:1-07F120:3, Mar. 2008.
[14] A. Masmoudi, A. Njeh and A. Elantably, "On the analysis and reduction of the cogging torque of a claw pole transverse flux permanent magnet machine," *Euro. Trans. Electr. Power*, vol.15, no.6, pp.513-526, Nov. /Dec. 2005.
[15] B.C. Mecrow, A.G. Jack and C.P. Maddison, "Permanent magnet machines for high torque, low speed applications," *in Proceedings of International Conference on Electrical Machines*, Vigo, Spain, pp.461-466, Sep. 1996.

Jia Xie He received the BS degree in electrical engineering from Xi'an Polytechnic University, Xi'an, China, in 1993, and the MS degree in electrical engineering from Xi'an Jiaotong University, Xi'an, China, in 2005. He is currently working towards the PhD degree in the electro-mechanical engineering from Xi'an Jiaotong University, Xi'an, China. His research interests are new electric machines, optimization techniques, advanced control strategies, and electric drive control system modeling.

Do-Hyun Kang He received the B.S. and M.S. degrees from Hanyang University, Seoul, Korea, in 1981 and 1989, respectively, and the Ph.D. degree from the Institute of Electric Machines, Traction and Drives, Technical University Braunschweig, Braunschweig, Germany, in 1996, all in electrical engineering. He was a Design Engineer in the Nuclear Power Plant at Hyundai Construction Company from 1981 to 1986. He is currently the Electric Propulsion Research Division of the Korea Electrotechnology Research Institute, Changwon, Korea. His research interests are magnetic levitation, linear drives, and new electric machines.

Byung-Chul Woo He received the B.S. degree in Mechanical engineering from Youngnam University in 1989, the M.S. and Ph.D. degrees in Mechanical Design from Kyungpook National University in 1991 and 2000. He is working mechanical design for electric machine in KERI. His research interests mechanical design of electric machine and actuator.

Ji-Young Lee She received the B.S., M.S, and Ph.D degrees in electrical engineering from Changwon National University, Changwon, Korea, in 2000, 2002, and 2006 respectively. Now she is with Electric Motor Research Center, Korea Electro-technology Research Institute, Changwon, Gyeongnam, Korea as a Senior Researcher. Her research interests are design and analysis of various electromagnetic devices by using finite element method, including permanent-magnet machines and transverse flux motors.

Zheng-Hui Sha He received the B.S. degree in Technique and Apparatus of Testing & Control at Xi'an University of Technology in 2006 and the MS in Mechanical Engineering at Xi'an Jiaotong University in 2010. Now he is a Ph.D student in Mechanical Engineering at Washington State University in U.S. Prior to his Ph.D study, much of his work has been primarily on the Machine Design, CAD and Structural Optimization; Dynamics and System Modeling & Simulation.

Sheng-dun Zhao He received the B.S. degree in mechanical engineering from Xi'an Jiaotong University, Xi'an, China, in 1983, and the M.S. and Ph.D. degrees in electro-mechanical engineering from Xi'an Jiaotong University, Xi'an, China, in 1986 and 1997, respectively. He was a winner of the First 100 Ph.D. Dissertations Competition of China in 1999. Since 1999, he has been a full Professor and Ph.D. supervisor. His research interests include advanced manufacture techniques and advanced control techniques.